İSTANBUL UNIVERSITY PRESS

Acta Infologica,
ACIN 2025, 9 (2): 719–744

https://doi.org/10.26650/acin.1830356
Submitted: 25.11.2025
Revision Requested: 07.12.2025
Last Revision Received: 16.12.2025
Accepted: 19.12.2025

Acta Infologica

Research Article

Open Access

Detection and Analysis of Out-of-Control Observations in Statistical Process Control Using Explainable Artificial Intelligence Models

Kenan Orçanlı [1] & Şükran Oruç [2]

[1] Istanbul Beykent University, Faculty of Arts and Sciences, Software Development Department, Istanbul, Türkiye
[2] Istanbul Beykent University, Faculty of Economics and Administrative Sciences, Department of Management Information Systems, Istanbul, Türkiye

Abstract Statistical process control (SPC) and anomaly detection are critical for enhancing product quality and operational efficiency in industrial manufacturing processes. However, traditional multivariate SPC methods cannot be directly applied to data with constant sum constraints, such as CoDa. In this study, the CoDa data obtained from the casting process were transformed into Euclidean space using the isometric log-ratio (ilr) transformation and monitored using the Hotelling T^2 control chart. Machine learning and explainability methods were employed to detect and understand the root causes of out-of-control signals. In this context, five classification models were compared: SVM, RF, XGBoost, logistic regression, and KNN. The highest test accuracy rate of 93.88% was achieved using the SVM model. To explain the decision mechanism of the model, SHapley Additive exPlanations (SHAP) and the Mason–Young–Tracy (MYT) generalization approach were jointly applied. The findings reveal that the SHAP and MYT results demonstrate a low level of consistency and that the model provides reliable local and global explainability outputs. By overcoming the limitations of traditional SPC methods, this integrated approach facilitates the understanding of root causes of anomalies in the casting process.

Keywords Statistical Process Control (SPC) · Anomaly Detection · Explainable Artificial Intelligence (XAI)

Citation: Orçanlı, K. & Oruç, Ş. (2025). Detection and Analysis of Out-of-Control Observations in Statistical Process Control Using Explainable Artificial Intelligence Models.. *Acta Infologica*, *9*(2), 719-744. https://doi.org/10.26650/acin.1830356

Corresponding author: Kenan Orçanlı kenanorcanli@beykent.edu.tr

INTRODUCTION

In today's manufacturing environments, increasing digitalization and global competition have made quality assurance and early warning mechanisms fundamental elements of sustainable competitiveness. In sectors such as chemistry and metallurgy with continuous production, the simultaneous monitoring of numerous quality variables increases the complexity of process control systems. Statistical process control (SPC) is an effective method that reduces process variability and ensures product quality (Cobb & Li, 2019). Multivariate methods, particularly Hotelling T^2 (Hotelling, 1947), provide a robust monitoring framework by combining multiple quality variables under a single statistic (Montgomery, 2020).

However, high-dimensional and structurally constrained data types determine the classical control charts' application limits (Aitchison, 1986). Compositional data (CoDa), such as alloy composition ratios commonly encountered in the casting industry, where all components are positive and their sum is constant, prevent the direct application of traditional multivariate methods (Boyles, 1997). Such data can be transformed into Euclidean space through the ILR transformation, enabling the application of multivariate process control methods (Imran, vd., 2023a; Vives-Mestres et al., 2014a; Vives-Mestres et al., 2014b). However, although these methods determine that the process is out of control, they remain insufficient in explaining the variables that caused the deviation. This situation, referred to as the "variable decomposition problem" in the literature, makes it difficult for process experts to make targeted improvement decisions (Montgomery, 2020).

The interest in machine learning-based models is increasing to overcome the limitations of classical methods (Wang & Chen, 2023). These models successfully solve pattern recognition and anomaly classification problems in high-dimensional data (Susto et al., 2015; Çınar et al., 2020). However, these models' internal workings are often characterized as a "black box" (Rudin, 2019). Explainable Artificial Intelligence (XAI) techniques are a critical tool for making the decision mechanisms of these models transparent (Arrieta et al., 2020; Gunning et al., 2021). The SHapley Additive exPlanations (SHAP) method provides local-level explainability by quantitatively revealing each prediction's variable contributions (Lundberg & Lee, 2017). By combining these contributions, the Mason–Young–Tracy (MYT) generalization approach enables the interpretation of the model's general tendencies at a global scale.

The primary objective of this study is to detect out-of-control signals in the casting process by analyzing compositional data obtained from the casting process using ILR transformation and machine learning-based models and to understand their root causes through explainability methods. Specifically, the following research questions will be addressed:

Which ML (machine learning) model demonstrates the highest classification performance after ILR transformation of compositional data?

When the SHAP and MYT methods are used together, are consistent and reliable results obtained in terms of model explainability?

What advantages does this integrated approach offer in identifying the root causes of anomalies in the casting process compared with traditional SPC methods?

The original contributions of the study can be summarized as follows: (i) implementation of machine learning and XAI integration for SPC applications in compositional data, (ii) provision of both local and global explainability through the combined use of SHAP and MYT methods, and (iii) presentation of a

practical application framework for the casting industry. This holistic approach significantly improves not only detection success but also the understanding of the root causes of deviations in the process.

COMPOSITIONAL DATA AND PROCESS MONITORING IN THE CASTING INDUSTRY

The brass alloy specific to the casting industry, which forms the foundation of the process control and anomaly detection problems addressed in the introduction section, and the CoDa (compositional data) structure that plays a critical role in this alloy, will be examined in detail in this section.

Casting industry and brass alloy production

The casting industry is one of the cornerstones of the manufacturing sector; it involves melting and pouring different metals and alloys into molds to shape them (Orçanlı, 2021). This method enables the economical and rapid production of single-piece parts with complex geometries. The quality of cast parts, which are widely used in strategic sectors such as automotive, defense, energy, and machinery manufacturing, largely depends on the preparation of metal alloys with the correct composition. Therefore, the continuous monitoring and control of alloy components in casting processes are vital for both product performance and process stability (Orçanlı et al., 2018; Orçanlı, 2021).

Brass alloys are common casting materials obtained by mixing elements such as copper (Cu) and zinc (Zn), along with lead (Pb), iron (Fe), and tin (Sn) in specific proportions (Özel, 2005). Typically containing 60-70% Cu and 30-40% Zn, these alloys are preferred in many industrial applications due to their ease of casting, corrosion resistance, good machinability, and esthetic appearance. However, the structure of such multicomponent alloys is determined not only by the presence of each element but also by the ratios of these elements to one another (Çalıgülü et al., 2023). This situation statistically places brass alloys within the scope of compositional data (CoDa).

Compositional data are data types with a constant sum (e.g., 100%) and positive values only. These structures are naturally defined within a simplex (S^D) space, and relative relationships between components are more meaningful than absolute values. For example, an increase in the zinc ratio in an alloy will automatically reduce the copper ratio; therefore, these ratios cannot be independently evaluated. Due to this characteristic, the direct application of classical statistical methods may lead to incorrect inferences and out-of-control situations (Aitchison, 1986). Instead, processes need to be monitored with CoDa-specific analysis approaches.

In metal mixtures with a compositional structure, such as brass alloys, the proportion of each element directly affects not only the chemical composition of the product but also its physical and mechanical properties, such as strength, ductility, hardness, and thermal conductivity (Çalıgülü et al., 2023). Therefore, even small alloy composition changes can lead to significant product quality differences. This reality reveals that compositional data are critically important in terms of quality control, product safety, functionality, and customer satisfaction.

Moreover, the consistency of the metal composition ratios is of great importance for the stability and repeatability of the production process (Özel, 2005). Variations in compositional data may occur under the influence of production parameters such as raw material purity variability, melting temperature, melting time, and furnace type. The timely and accurate detection of these deviations prevents defective production and reduces costs (Sakalli & Birgoren, 2008; Baykoç & Sakallı, 2009). In this context, process monitoring systems structured with the CoDa approach not only detect anomalies but also provide advanced decision

support to the casting industry with the capacity to analyze which element causes these anomalies (Vives-Mestres et al., 2014a; Zaidi et al., 2019). This situation clearly demonstrates how the process-based fundamental representation methodology can be enriched with compositional data, the absence of which is felt particularly in process industries.

In conclusion, the correct determination, monitoring, and control of element ratios used in the production of metal alloys such as brass in the casting industry are fundamental requirements for the sustainability of product quality, process reliability, and customer satisfaction. Therefore, the ability to analyze compositional data in a statistically meaningful manner is considered a strategic competency that provides a competitive advantage within the modern manufacturing paradigm.

Compositional data

Compositional data (CoDa) are multivariate data types with a constant sum constraint on their components. Such data are typically presented in the form of percentages, frequencies, or proportions and only consist of positive components. They are widely used in many sectors, particularly in the food, medical, and chemical industries (Aitchison, 1986). The unique characteristics of CoDa require approaches different from those of classical statistical analysis methods. The control of CoDa in the context of statistical process control (SPC) is receiving increasing attention, and studies on the development of various control charts in this field are on the rise.

Boyles (1997) first attempted to control CoDa, proposing a chi-square control chart using the properties of the Dirichlet distribution. Research on the development of different control charts for monitoring CoDa continued in subsequent years. Vives-Mestres et al. (2014a) proposed an individual Hotelling T^2 control chart for CoDa, and the same research team (Vives-Mestres et al., 2014b) conducted a study on the interpretation of out-of-control signals in three-component CoDa. In addition, Tran et al. (2018) presented a new approach in CoDa control by developing a Markov chain-based MEWMA control chart.

Research aimed at increasing the applicability of CoDa in statistical process control has focused on examining the effect of measurement errors on the performance of control charts. Zaidi et al. (2019, 2020) evaluated the performance of the Hotelling T^2 control chart and MEWMA control chart for CoDa under measurement errors. In this context, the effects of measurement errors on process monitoring directly affect the reliability of control charts, and an in-depth examination of this issue is of great importance.

In recent years, studies on control charts developed for CoDa have focused on examining the parameter estimation of the MCUSUM control chart and the effect of measurement errors on this chart Imran et al. (2022a, 2023b). Additionally, the effect of variable sample size on the MEWMA control chart has been investigated, and the effects of variable sampling intervals on the zero-state and steady-state performance of the MEWMA control chart for CoDa have been examined in detail (Imran et al., 2023c; Imran et al., 2022b). Furthermore, Imran et al. (2023a) evaluated the performance of the variable sampling interval Hotelling T^2 control chart in the presence of measurement errors.

Zaidi et al. (2019, 2020) proposed a new model to more precisely identify out-of-control situations encountered during the monitoring of CoDa. This study developed a pattern recognition approach based on multilayer feedforward ANNs. Within the scope of the simulation studies, six different models were used to trigger changes and trends in CoDa, and the generated data were subjected to isometric log-ratio transformation. The Hotelling T^2 statistic obtained from the transformed data was made suitable for the pattern recognition model using the backpropagation learning algorithm. The results reveal that the

proposed model demonstrates high accuracy in detecting patterns in control charts, particularly in cases of out-of-control situations.

These studies make important contributions to the improvement of existing methods and the development of new methods for the control of CoDa. Developments in the related literature reveal theoretical and practical advances aimed at enabling the more effective use of CoDa in SPC applications. Future research in this field is anticipated to be shaped particularly toward reducing measurement errors and making control charts more sensitive.

A (1×p) row vector $y = (y_1, ..., y_p)$ is a p-component CoDa vector if it belongs to the simple sample space S^p and satisfies the following condition:

$$S^p = \{ y= (y_1 , ... , y_p)| \, y_i >0 \, , i = 1,2,...,p \text{ and} \sum_{i=1}^{p} y_i = \kappa \tag{1}$$

Here, $\kappa > 0$ is a constant value that can take different values. If CoDa consists of proportions, $\kappa = 1$, and if it consists of percentages, $\kappa = 100$.

Two compositions may be numerically different but can carry the same relative information using the closure function (C), i.e., C(y) = C(z). This function is defined as follows:

$$C(y) = (\frac{\kappa \, y_1}{\sum_{i=1}^{p} y_i}, \quad \frac{\kappa \, y_2}{\sum_{i=1}^{p} y_i}, ..., \frac{\kappa \, y_p}{\sum_{i=1}^{p} y_i} \tag{2}$$

Aitchison (2011) defined a special geometry for CoDa and developed new operators for adding CoDa vectors and multiplying a CoDa vector by a scalar magnitude. The perturbation operator $\oplus$, which performs the addition of CoDa vectors, $y \oplus z = C(y_1 z_1, \; y_2 z_2, \; ..., \; y_p z_p)$,, creates a new vector obtained from the multiplication of each component of these vectors. This operator creates a new CoDa vector by mutually multiplying the components of two CoDa vectors. This operation is particularly important in the analysis process while preserving the compositional structure of multivariate data within the Aitchison geometry framework. The perturbation operator provides a practical way to model the interaction of different CoDa vectors.

The powering operator $\otimes$, $a \otimes y = C(y_1^a, \; y_2^a, \; ..., \; y_p^a)$, transforms a CoDa vector by raising each component to a constant power. This operation is widely used in scaling CoDa data and allows each data component to be proportionally amplified. The use of the powering operator is particularly important for examining the general behavior of CoDa vectors and ensuring that certain components carry greater weight.

There are two fundamental methods for handling CoDa data. The first method involves performing operations using perturbation and powering operators within the Aitchison geometry. Aitchison geometry is a special mathematical framework used in CoDa analysis, enabling different statistical calculations to be performed while preserving the true ratios of the data. This method was developed to overcome the challenges encountered in the direct application of classical statistical methods in the analysis of CoDa data.

The second method involves transforming the data into log-ratio coordinates. This transformation facilitates easier data processing by converting CoDa vectors from the simplex space (specifically the space where multivariate ratios exist) to real space. While this transformation allows the use of classical statistical techniques, it also facilitates data interpretation. Log-ratio coordinates create a more suitable environment for statistical modeling and analysis by revealing the relationships among the fundamental components of CoDa. Once statistical analyses are performed, the data can be transformed back to the simplex space during the interpretation phase if necessary, allowing interpretation in accordance with the original data format.

To date, a series of log-ratio coordinate representations related to these two methods have been developed. These representations are used to analyze the different properties and structures of CoDa more efficiently and enable accurate data interpretation. Such log-ratio transformations allow CoDa to be subjected to more comprehensive statistical evaluations and enable more meaningful use of data in various industries, particularly in food, chemistry, and medicine.

Several log-ratio coordinate representations have been introduced. One of these is the CLR transformation, defined as follows:

$$\mathrm{clr(y)} = (\ \ln \frac{\mathrm{y_1}}{\overline{\mathrm{y_{GM}}}}\ , \ln\frac{\mathrm{y_2}}{\overline{\mathrm{y_{GM}}}}\quad ,\ldots\ldots, \ln\frac{\mathrm{y_p}}{\overline{\mathrm{y_{GM}}}} \tag{3}$$

Here, $\overline{\mathrm{y_{GM}}}$ is the row-wise geometric mean of y:

$$\overline{\mathrm{y_{GM}}} = (\prod_{\mathrm{i}=1}^{\mathrm{p}} \mathrm{y_i})^{\frac{1}{\mathrm{p}}} = \exp\left(\frac{1}{\mathrm{p}}\sum_{\mathrm{i}=1}^{\mathrm{p}} \ln\ \mathrm{y_i}\right) \tag{4}$$

The isometric log-ratio (ILR) transformation for composition is another log-ratio coordinate representation, which is defined as follows:

$$\mathrm{ilr(y)}{=}\mathrm{y}^* = \mathrm{clr(y)B^T} \tag{5}$$

Here, Ψ is a matrix of dimensions (p–1, p) for binary ILR partitioning and can take different values (Pawlowsky-Glahn et al., 2015). The matrix used in this study is as follows:

$$B_{i,j} = \begin{cases} \sqrt{\frac{1}{(d-i)(d-i+1)}} & j \le d-i \\ -\sqrt{\frac{d-i}{d-i+1}} & j = d-i+1 \\ 0 & j > d-i+1 \end{cases} \tag{6}$$

The inverse ILR transformation is defined as follows:

$$\mathrm{ilr^{-1}}\ \ (\ \mathrm{y}^*) = \mathrm{y} = \mathrm{C(\exp(y^*\ B))} \tag{7}$$

The ILR transformation preserves the geometric structure of CoDa by mapping the original data to a space consisting of additive and independent components. This characteristic can be beneficial in constructing multivariate control charts for CoDa, as the ILR transformation's isometric properties can facilitate the interpretation of patterns and variations in the data. Although additive log-ratio (ALR) and centered log-ratio (CLR) transformations can also be used for control charts on CoDa, they do not preserve the data's geometric structure in the same way as the ILR transformation. Therefore, these transformations may result in less accurate or reliable control charts, especially when performing multivariate data analysis. Therefore, the ILR transformation is generally accepted as the preferred approach for constructing multivariate control charts on CoDa. The closed column-wise geometric mean of y is used to measure the central tendency of CoDa, that is:

$$\mathrm{cen(y)}{=}\overline{\mathrm{GM}} = \mathrm{C}[\overline{(\mathrm{GM})}(1),\ldots\ldots\ldots, \overline{\mathrm{GM}}(\mathrm{p})] \tag{8}$$

$$\overline{\mathrm{GM_j}} = (\prod_{\mathrm{i}=1}^{\mathrm{n}} \mathrm{y_{i\,j}})^{\frac{1}{\mathrm{n}}}\ \ \mathrm{j}{=}1,2,\ldots\ldots\ldots,\ \mathrm{p} \tag{9}$$

According to Aitchison [4], the variation of the compositional data (CoDa) is defined as follows:

$$V{=}\begin{bmatrix} \mathrm{v_{1\,1}} & \cdots & \mathrm{v_{1\,p}} \\ \vdots & \ddots & \vdots \\ \mathrm{v_{p\,1}} & \cdots & \mathrm{v_{pp}} \end{bmatrix}$$

Here,

$$v_{ij} = \mathrm{var}(\ln(\frac{y_i}{y_j})) \tag{10}$$

The normalized variation matrix also represents the dispersion in the CoDa data, i.e.,

$V^* = \begin{bmatrix} v^*_{11} & \cdots & v^*_{1p} \\ \vdots & \ddots & \vdots \\ v^*_{p1} & \cdots & v^*_{pp} \end{bmatrix}$

Here,

$$v^*_{i,j} = \mathrm{var}(\frac{1}{\sqrt{2}}\ln(\frac{y_i}{y_j})) \tag{11}$$

Here, *V* and V^* are symmetric matrices with zero diagonal terms. Total variance is used to measure the overall dispersion of CoDa data. The total variance of CoDa is expressed as follows:

$$\mathrm{Tvar}(y) = \frac{1}{2p}\left(\sum_{i,j=1}^{p} \mathrm{var}\left(\ln\left(\frac{y_i}{y_j}\right)\right) = \frac{1}{2p}\left(\sum_{i,j=1}^{p} v_{i,j}\right) = \frac{1}{n}\sum_{k=1}^{n} d_a^2\left(y_k, \overline{GM}\right); \tag{12}$$

Here, the expression $d_a^2\left(y_k, \overline{GM}\right)$ is also known as metric variance because it represents the mean of squared distances.

HOTELLING T² CONTROL CHART AND ANOMALY DETECTION MASON-YOUNG-TRACY DECOMPOSITION METHOD

Hotelling *T²* control chart and anomaly detection

The Hotelling *T²* control chart is a fundamental statistical method for monitoring and controlling multivariate processes. The statistic used in this control chart measures the distance of observation vectors from the process mean under the assumption of a multivariate normal distribution. Mathematically, Hotelling *T²* is calculated considering the sample size, process mean, and covariance matrix, and can be defined as the univariate Student's t-test's multivariate extension. Thus, multiple quality characteristics are combined into a single statistical measure, enabling the early detection of possible deviations in the process.

The Hotelling *T²* control chart only has an upper control limit (UCL) because the *T²* statistic is a quadratic expression and cannot take negative values. The *T²* values of process observations are compared with this upper limit to determine whether the process is in control. High *T²* values indicate shifts in the process mean or deviations in the variance structure, and this situation is considered an out-of-control signal. However, since this signal does not directly indicate which variables are causing the problem, decomposing the signal source is difficult.

Many methods have been developed in the literature to address the problem of identifying the signal source. The PCA method expresses Hotelling *T²* as the sum of independent squares of principal components using eigenvalue decomposition of the covariance matrix. In this way, the contribution of each component to the deviation in the process can be examined. However, the fact that principal components are linear combinations of the original variables complicates the interpretation process.

The Bonferroni simultaneous confidence intervals method provides clues about the component from which the signal originates by using confidence intervals for the mean values of the variables. Although this method provides statistical protection against the multiple testing problem, it assumes that the variables

are independent. Additionally, the integrated graphical presentation of multivariate and univariate control charts helps to more clearly identify the variables causing the error.

Regression-based analyses are used to model the complex covariance relationships between variables and create control charts for residuals, which are the differences between observed and regression-predicted values. In this way, the variable from which the signal originates can be more precisely detected. The Mason-Young-Tracy (MYT) decomposition method decomposes the Hotelling T^2 statistic both on a variable basis and in terms of the appropriateness of the inter-variable relationship to the data structure, providing more comprehensive information about the signal's origin.

However, some methods have limitations in terms of practical applicability due to computational complexity in high-dimensional data structures. For example, although testing all subsets reduces uncertainty, it creates difficulties in terms of computational cost and calculation times. Therefore, signal interpretation in MPC should be performed through combinations of different techniques and selections appropriate to the application context.

In conclusion, although Hotelling T^2 control charts are a powerful tool for monitoring the general state of multivariate processes, they remain insufficient in explaining the signal source. Therefore, multivariate process control approaches supported by signal interpretation techniques and decomposition methods are critical for process reliability and decision support mechanism effectiveness.

Artificial intelligence-based approaches are gaining increasing importance to overcome the limitations of classical multivariate process control techniques in signal decomposition and capture complex, high-dimensional patterns in process data. However, the "black box" structures of deep learning (DL) models lead to interpretability and reliability issues in industrial applications. To address these problems, explainable artificial intelligence (XAI) methods such as SHAP (SHapley Additive exPlanations) and LIME (Local Interpretable Model-agnostic Explanations) are used techniques reveal the variable effects underlying model decisions in a transparent and mathematically consistent manner, facilitating the interpretation of model outputs by engineers and decision-makers. Thus, the combined use of classical statistical methods with AI-based explainable models provides significant advances in the accuracy, flexibility, and explainability of decision support mechanisms in multivariate process control.

Mason-Young-Tracy (MYT) decomposition method

The Mason-Young-Tracy (MYT) method is a powerful technique that, when a signal occurs in multivariate T^2control statistics, diagnoses the source of this signal by decomposing it into unconditional (individual variable) and conditional (inter-variable relationships) components (Özel, 2005). The general steps of this procedure are as follows:

Decomposition of the T^2 *Statistic:* The general T^2 statistic ($T^2=(X-\overline{X})' S^{-1}(X-\overline{X})$)can be decomposed into two independent terms: $T^2=T_1^2+T^2_{p|1,2,....p-1}$

Unconditional Term (T_1^2)*:* Indicates that a single variable (for example, X_1) is out of control. Simply put, it measures how far the corresponding variable deviates from its mean, which is essentially a normalized squared deviation.

Conditional Term ($T^2_{p|1,2,....p-1}$)*:* Represents how much a variable (X_p), deviates from its regression-based prediction given the other variables (X_1,...,X_{p-1}). This deviation indicates a disturbance in the variables' relationships. The calculation of the conditional term involves regression coefficients (e.g.,$B_p^{'}$)

Signal Detection and Critical Thresholds:

To determine whether a signal is present, each computed unconditional and conditional component is evaluated against the pre-specified critical limits.

For the Unconditional Term: UT=$\left(\frac{n+1}{n}\right)F_{(\alpha,1,n-1)}$

For the Conditional Term: CT=$\left(\frac{(n+1)(n-1)}{n(n-k-1)}\right)F_{(\alpha,1,n-k)}$ A term exceeding its critical value is considered evidence of a process anomaly (signal).

Fault Diagnosis Algorithm: MYT employs an iterative algorithm to systematically identify the signal's origin:

Step 1: Examine the unconditional terms (T_i^2) of all variables are examined. Individual variables that signal (i.e., those that are problematic on their own) are identified and removed from the analysis.

Step 2: The bivariate conditional terms ($T_{i|j}^2$) among the remaining variables are analyzed. The signaling variable pairs (i.e., those with problems in their relationships) are identified and removed.

Subsequent Steps: Similarly, trivariate, quadrivariate, and higher-order conditional terms are examined sequentially for the remaining variables.

This process continues until no signal remains or until all variables/groups have been analyzed.

The MYT method rapidly and effectively identifies the specific cause underlying the T^2 signal (whether individual variable anomalies or disturbances in complex variable relationships) to make the process more comprehensible.

MACHINE LEARNING AND EXPLAINABILITY METHODS

Support vector machine

Support vector machines (SVMs) are powerful algorithms that are widely used in the field of machine learning for supervised classification and regression problems. SVMs possess a high generalization ability (Cortes & Vapnik, 1995). Based on the maximum margin principle, SVM constructs an optimal hyperplane that separates observations belonging to different classes with the widest safety margin (Vapnik, 2013). This methodology maintains its effectiveness not only in linearly separable datasets but also in high-dimensional data structures that are not linearly separable through kernel functions (kernel trick) (Boser et al., 1992). This approach facilitates separability by nonlinearly mapping the data into higher-dimensional feature spaces (Müller et al., 2018). The curse of dimensionality problem, frequently encountered in multivariate control charts, can be significantly mitigated when integrated with tensor decomposition technologies.

Random forest

RF is a flexible and effective ensemble learning algorithm that is fundamentally composed of classification and regression trees (Breiman, 2001). Based on the bagging (bootstrap aggregation) method (Breiman, 1996), this algorithm can offer solutions to both classification and regression problems. When constructing a RF model, training sets are first created through the bootstrapping method. Subsequently, a separate decision tree is built in parallel for each training set. The most suitable features are used from among all available features in splitting the nodes of each decision tree. This process offers an effective method for separating hidden information within large datasets (Cutler et al., 2012).

The general workflow of the RF algorithm can be summarized as follows:

Input Parameters: The algorithm reads parameters such as the training set (T), algorithm features (F), and number of trees in the forest (K).

Probability Set: Create an initial empty probability set (P).

Bootstrapping: The bootstrapping process is performed for the training set.

Iterative Tree Formation: Within a loop, the function designed for random tree learning executes operations by partitioning the tree into subsets based on the input training set and algorithm features, and generates probabilities for each subset.

Combination of Probabilities: The generated probabilities are added to the probability set, and the loop is completed.

Optimal Split: The most suitable subset (f) among the resulting subsets (the one yielding the minimum error) is found and split according to the best feature.

Final Result: The final algorithm result (classification or regression value) is returned.

In this study, the RF's ensemble learning structure was leveraged to increase the model's stability and achieve high prediction accuracy (Liaw & Wiener, 2002).

XGboost

The Extreme Gradient Boosting (XGBoost) algorithm, developed by Chen and Guestrin (2016), is an optimized variant of the gradient boosting algorithm. This algorithm has gained wide acceptance in data mining and statistical learning and has demonstrated remarkable performance on competitive data science platforms since its publication. Chen and Guestrin (2016) reported that 58.6% of the 29 data science competitions held on the Kaggle platform in 2015 were won using XGBoost.

The main methodological and computational advantages of XGBoost over traditional gradient boosting methods are as follows:

Tree Pruning Strategy: The algorithm uses a maximum depth parameter to prevent over-complexity and performs systematic pruning to minimize overfitting.

Enhanced Loss Function Optimization: While traditional methods use first-order derivative information, XGBoost incorporates second-order derivative (Hessian matrix) information, resulting in a more precise and efficient optimization process.

Parallel Processing Architecture: XGBoost can effectively utilize multi-core processors due to its parallel computing capability. This feature ensures scalability by significantly increasing the computational efficiency when large datasets are used.

These methodological advantages position XGBoost as a powerful algorithm in terms of both high prediction accuracy and computational efficiency, making it a critical tool in modern ML applications. In this study, XGBoost's high performance and speed capabilities were the reason for our choice to obtain fast and accurate results on our large dataset.

Logistic regression

Logistic regression is a statistical model used for categorical (binary or multinomial) rather than numerical dependent variables. Unlike normal linear regression, this model calculates the probability of the output (Y_i) (0≤E(Y_i)≤1)and extends this limited range to the infinite range (−∞,∞) using the logit transformation.

The model coefficients are estimated using the maximum likelihood method, and the significance of these coefficients is tested using the Wald test. The logistic regression results are interpreted using the odds ratio (OR), which represents the “ratio of the probability of occurrence to the probability of non-occurrence.” An OR greater or less than 1 associated with a change in a factor indicates the increasing or protective effect of this factor on the outcome variable (Yavuz & Çilengiroğlu, 2020).

The k-nearest neighbor

The k-nearest neighbor (kNN) algorithm is a simple yet effective ML method used in classification and regression problems. This algorithm examines the class labels of the k nearest neighbors in the training set and makes a prediction based on these labels when classifying a new data point. The majority decision of the nearest neighbors determines the class of a data point. Different distance metrics, such as Euclidean, Manhattan, Minkowski, and Chebyshev, can be used for neighborhood calculation in this method. One of the greatest advantages of kNN is that it does not require the construction of a complex model in advance and can dynamically adapt as new data arrive (Dilki & Başar, 2020).

SHapley additive exPlanations (SHAP)

Lundberg and Lee (2017) first developed the SHapley Additive exPlanations (SHAP) approach. This method quantitatively evaluates the effects of data elements, features, or variables that contribute to a model's prediction. The SHAP algorithm is an analytical approach based on cooperative game theory that was developed to explain the output of a machine learning model (Mihirette & Tan, 2022).

The field of Explainable Artificial Intelligence (XAI) aims to dissolve the "black box" nature of machine learning and deep learning models, making their prediction mechanisms more transparent and interpretable. In this context, the SHapley Additive exPlanations (SHAP) algorithm is recognized as one of the leading methodologies for the detailed analysis of model outputs and, particularly, for interpreting individual predictions.

From a game-theoretic perspective, the SHAP algorithm systematically reveals the extent to which each feature (variable) contributes to a model’s prediction process. This approach offers an effective tool, especially in multivariate statistical process control applications and in examining the root causes of unusual observations (anomalies) detected by the Hotelling T^2statistic. Thus, the variable(s) that most influenced the anomalous behavior of a specific observation can be determined quantitatively and clearly using SHAP values.

The SHAP algorithm’s theoretical framework is based on the Shapley value concept, developed in the cooperative games branch of game theory (Shapley, 1953). In the game theory literature, the Shapley value represents the fair distribution of each player’s contribution to the total payoff in a multi-player game. Similarly, in the SHAP approach, each feature is treated as a "player in the game," and its marginal effect on the model prediction is measured by the corresponding Shapley value.

Unlike classical importance ranking methods, this allows SHAP to account not only for the direct effect of a single variable but also for the interactional contributions between variables. In this respect, SHAP offers a very powerful methodology for interpreting both linear and complex nonlinear models.

To determine the marginal contribution of each feature, the SHAP algorithm examines all possible feature combinations, including and excluding the relevant feature. The core principle is to calculate the difference in model performance between the presence and absence of a particular feature. Because of this systematic process, the Shapley contribution value (ϕ_i) for each feature is obtained. Mathematically, the SHAP value is defined as follows (Lundberg et al., 2018):

$$\emptyset_i = \sum_{S \subset F \setminus \{i\}}^{n} \frac{|S|!(F - |S| - 1)!}{|F|!} \left[g_{s \cup \{i\}} \left(x_{s \cup \{i\}} \right) - g_s \left(x_s \right) \right] \tag{13}$$

In this formulation:

F: the set of all features,

i: denotes the i-th feature whose contribution is calculated,

S: any subset of set F, excluding feature i,

f_x(S∪{i}): denotes the model prediction obtained by including feature i,

f_x(S): prediction obtained solely with subset S, excluding feature i.

The advantage of the SHAP algorithm is its ability to simultaneously provide both local (on a single observation basis) and global (on an entire dataset basis) explainability of the model. Using SHAP values, especially in high-dimensional datasets, allows for the detailed analysis of

The variables that play a critical role in anomaly detection

Justifications by which the model classified or predicted a particular observation

How inter-variable interactions are reflected in the model output.

Due to these features, SHAP stands out as a critical XAI tool that ensures reliability, transparency, and auditability in academic studies and industrial applications.

METHOD AND RESEARCH FINDINGS

Analysis method

This study presents an innovative process monitoring and anomaly detection method for CoDa obtained from casting processes. The CoDa data were transformed into the Euclidean space using the isometric log-ratio (ilr) transformation to overcome the limitations of classical multivariate analysis methods. Subsequently, the Hotelling T^2 control chart was applied to detect out-of-control process states. To enhance the method's capacity for in-depth understanding of the anomaly origins, various ML models, such as support vector machines, random forest, XGBoost, and artificial neural networks, were trained and compared. Additionally, the SHapley Additive exPlanations (SHAP) method and the Mason–Young–Tracy (MYT) generalization approach were used in an integrated manner to ensure the transparency of the decision mechanism of the model. This integrated approach strengthens both the anomaly detection performance and the interpretability of decision processes by comparing the SHAP contributions with the MYT results.

The application production process

The application area of this study is the production subprocess of the Brass Factory Directorate of the Machinery and Chemical Industry Institution (MCII). This process encompasses the manufacturing of cartridge cups, case and jacket blanks, and driving bands to meet military requirements, as well as the

production of brass, lead, and aluminum alloys. Brass alloy, in particular, is critically important for industrial and military applications. It is obtained through controlled casting processes involving copper (Cu), zinc (Zn), and sometimes elements such as lead (Pb). The production subprocess consists of three main sections: the Weighing Preparation, Raw Material Melting and Casting, and Extrusion and Cupping sections. The factory's primary production item, MS 58 type brass alloy, is manufactured in compliance with DIN 17660 standards, and its constituent elements' weight percentages are maintained within strict specification ranges. Any element falling outside the predetermined limits leads to the scrapping of the product. This alloy is used in critical industrial and military applications.

In metallurgical production processes, especially in the manufacturing of alloys such as brass, assuring product quality is critical. This process typically begins with spectral analysis, in which the elemental composition of the molten metal is examined and its compliance with the DIN standards is checked. The deviations in the element ratios are corrected by adding appropriate substances to the furnace. For instance, if the ratio of a specific element is below the reference value, the missing substance is added; if it is above the reference value, balancing substances such as pure zinc or copper are introduced to bring the ratios to the ideal level. When transitioning to a different product during continuous production, pure zinc or copper is again used to adjust the level of impurities remaining from the previous casting to the new product's specifications. This detailed control and adjustment process is applied separately for each induction furnace, and the holding furnaces homogenize the molten metal. In the final stage, physical properties such as the hardness, diameter, and length of randomly selected metal bars are inspected, and nonstandard products are scrapped and returned for reprocessing. This three-stage quality control process ensures a continuous and rigorous monitoring mechanism at every step from production to the final product.

Any deviation in the production process causes a deviation from specification ranges, leading to the scrapping of the products. Therefore, process control and anomaly detection are vital for maintaining product quality and production efficiency.

Application Data, Methods, and Limitations

In this study, 351 real production data points for MS 58 brass alloy were obtained from the production subprocess of the Machinery and Chemical Industry Institution (MKEK) Brass Factory Directorate. Data were sourced from the article prepared by Orçanlı (2021). The alloy's quality is defined by its chemical composition, where the weight percentages of the main and additive elements, such as copper (Cu), zinc (Zn), lead (Pb), iron (Fe), tin (Sn), aluminum (Al), nickel (Ni), and antimony (Sb), constitute the fundamental quality control parameters. The requirement that each element must remain within the lower and upper specification values stipulated by DIN 17660 standards is critical for final product quality; deviations from these limits lead to the product being considered defective.

The application data are characterized as compositional data structures (CoDa), meaning that their components are interdependent and sum up to a specific constant, restricting the direct application of standard multivariate statistical techniques. To overcome this limitation, the data were transformed into Euclidean space using the ILR transformation. This transformation provides a structure where standard statistical analyses can be performed by eliminating the dependent relationship between the variables and preserving the variance-covariance structure. For the ILR transformation to be applicable, zero-valued observations in the dataset were replaced with a positive, yet minimal, value to prevent errors that might arise from the logarithmic transformation. The pandas (data manipulation), numpy (scientific computations), and

scikit-bio (specialized functions for ILR transformation) libraries of the Python programming language were utilized in this transformation process.

The limitations of this study primarily stem from the dataset's source, nature, and distribution characteristics. The use of data from past periods restricts the real-time monitoring of dynamic changes or the rapid adaptation to unforeseen sudden deviations in current production processes. Furthermore, the dataset only includes the chemical composition features of the MS 58 brass alloy, which prevents direct inference about other alloy types produced by the MKEK brass factory directorate or potential sources of anomalies in different production stages. This situation limits the generalizability of the developed model and narrows the direct applicability of the findings to similar but different production lines or products. Additionally, while class imbalance in the test dataset is a significant limitation affecting model performance, it is meaningful in that it reflects real operational conditions. Despite this imbalance, the cross-validation results applied within the scope of the study were internally evaluated during model development and serve as supportive evidence for evaluating the overall validity of the model. Future studies aim to mitigate the class representation imbalance by creating a more balanced test dataset. This approach ensures methodologically sound progress in compliance with academic standards.

The phase I sample size (n = 25) is below the commonly recommended threshold (n > 50) for 7-dimensional multivariate control charts. This constraint reflects the practical difficulty of obtaining extended periods of verified in-control production in dynamic casting operations. This limitation may affect the stability of the estimated covariance matrix and control limits. Future studies should aim to establish larger Phase I datasets through longer monitoring periods or pooled data from multiple production campaigns.

Transformation of raw data into CoDa data

The compositional dataset used in the study consists of eight components found in brass alloys: Cu, Pb, Fe, Sn, Al, Ni, Sb, and Zn. Given that the constant sum constraint (100%) inherent in compositional data leads to spurious correlations and a singular variance–covariance matrix in classical multivariate methods, the data were subjected to the Isometric Log-Ratio (ILR) transformation.

Within this scope, the components were first normalized through a closure operation to ensure that row sums equaled 1. To establish the mathematical validity for subsequent logarithmic operations and prevent ln(0) issues, we imputed zero values in the dataset using a robust pseudo-count of 10^{-6}. Subsequently, the CLR transformation was applied. The centering property of the CLR transformation was verified by confirming that the mean of the transformed components was effectively zero (e.g., the CLR_Fe mean was −0.247).

Table 1:

Log-ratio contrasts of ILR components for the brass alloy dataset

ILR Component	Positive group (numerator)	Negative (Denominator) group	Log-ratio Contrast Represented
ILR_1	{Cu}	{Pb}	Log-ratio between Cu and Pb concentrations
ILR_2	{Cu,Pb}	{Fe}	Log-ratio between the geometric mean values of Cu,Pb and Fe
ILR_3	{Cu,Pb,Fe}	{Sn}	Log-ratio between the geometric mean of Cu,Pb,Fe, and Sn
ILR_4	{Cu,Pb,Fe,Sn}	{Al}	Log-ratio between the geometric mean of {Cu,...,Sn} and Al

ILR Component	Positive group (numerator)	Negative (Denominator) group	Log-ratio Contrast Represented
ILR_5	{Cu,...,Al}	{Ni}	Log-ratio between the geometric mean of {Cu,...,Al} and Ni
ILR_6	{Cu,...,Ni}	{Sb}	Log-ratio between the geometric mean of {Cu,...,Ni} and Sb
ILR_7	{Cu,...,Sb}	{Zn}	Log-ratio between the geometric mean of {Cu,...,Sb} and Zn

Finally, the CLR vectors were converted to ILR coordinates using an orthogonal transformation matrix (Ψ). This Ψ matrix was constructed based on the SBP using the Gram–Schmidt orthonormalization process. The ILR transformation successfully reduced the eight-component dataset to seven independent variables, consistent with the D–1 rule, thereby eliminating spurious correlations. An inverse transformation test with a negligible reconstruction error (2.33×10^{-15}) confirmed the accuracy of this mapping.

The correlation matrix computed in the ILR space validated the orthogonal and independent structures of the transformed variables. The internal variability within the dataset was quantitatively revealed using the D × D dimensional variation matrix (V). This matrix identified the lowest variance (0.0033) between Cu and Zn, suggesting a tight, inverse relationship between these two major components. Conversely, the highest contrast (18.8716) was observed between Al and Sb, indicating that the variation between these components is unconstrained. The total variance calculated in the log-ratio space (= 17.279580) provided a scalar summary of the dataset's overall natural variation, confirming that the ILR transformation is a valid and preferred methodology for examining compositional data's structural properties (Table 1).

Multivariate Outlier Analysis

The Mahalanobis distance and Hotelling's T^2 statistics were used to detect multivariate outliers in the compositional dataset. The analysis was conducted using a two-phase procedure. The first 25 observations from the dataset were designated as the reference group in the first phase (Phase 1). This group represents the presumed in-control and normally distributed state of the process. The mean vector (μ) and the variance-covariance matrix (Σ) were calculated using this reference group, and these values were compared with other observations in the dataset. In Phase 1, the reference group was checked for outliers, and no outliers were detected, indicating that the reference group was homogeneous and consistent. In the second phase (Phase 2), the Hotelling's T^2 statistic was calculated for the entire dataset (326 observations) using the μ and Σ values obtained from Phase 1, and the multivariate distance of each observation from the reference group was measured.:

$$T^2 = (x_i - \mu)^T \Sigma^{-1} (x_i - \mu) \tag{14}$$

Here, x_i represents the observation under examination, μ represents the reference group mean, and Σ^{-1} represents the inverse of the variance-covariance matrix. The resulting T^2 values were compared with the chi-square distribution to identify outliers. A threshold value of 25.0114, corresponding to a 0.95 probability level ($p<0.05$), was used, and observations with a T^2 value above this threshold were classified as outliers. This approach allows for an accurate and consistent outlier detection for the entire dataset in Phase 2 owing to the established reliable reference basis in Phase 1.

Construction of Hotelling's T² control chart with compositional data and outlier detection

In this study, a compositional data (CoDa)-based multivariate Hotelling's T^2 control chart was employed to assess whether the control process is statistically significant. Prior to the analysis, the compositional data were transformed using the ILR to remove the closure constraint (i.e., the sum of k components being constant) and enable data processing in Euclidean space. Hotelling's T^2 analysis was performed on p = 7 new variables obtained from this transformation. The Hotelling's T^2 control chart was established using a two-phase approach to monitor the process and detect potential outliers.

Table 2:

Mean Vector and Covariance Matrix of Phase 1 Data

Variable	Mean ($\bar{x}$)
ILR_1	2.468146
ILR_2	4.099544
ILR_3	1.934564
ILR_4	11.123647
ILR_5	0.890975
ILR_6	6.306278
ILR_7	-6.729896

The statistical parameters forming the basis of the analysis were derived from Phase 1 data, where the process was assumed to be stable. In this context, the first n=25 observations from a dataset consisting of a total of N=351 observations were designated as Phase 1 data. Whether the Phase 1 data contained outliers was tested using the Mahalanobis distance method with the χ^2 distribution, and no outliers were detected. The χ^2 threshold value used in this analysis was determined as 18.4753. The fundamental statistical parameters (mean vector and covariance matrix) calculated using the Phase 1 data are presented in Table 2.

Additionally, the 7×7 variance-covariance matrix (S) obtained from the Phase 1 data was used in the UCL calculation. The UCL used to monitor Phase 2 data was calculated at a 95% confidence level (α=0.05) based on the F distribution using the following formula:

$$\mathrm{UCL}= \frac{1}{n_1(n_1-p)} p(n_1+1)(n_1-1)F_{\alpha,\, p,\, n_1-p} \tag{15}$$

UCL : Upper control limit

n_1 : Sample size of Phase 1

P : Number of variables in the analysis

α (Alpha) : Significance level or Type I error probability (α)

$F_{\alpha,\, p,\, n_1-p}$: The critical value is read from the F-distribution table. Here, p denotes the degrees of freedom and n_1-p is the denominator degrees of freedom.

Using this formula with n = 25 and p = 7, the UCL value was determined to be 25.0114. The calculated UCL value was applied to the remaining m = 326 Phase 2 observations (observations 26–351). The T^2 values for each phase 2 observation indicate the deviation magnitude from the phase 1 mean vector. Because of the analysis, a total of 65 observations in the Phase 2 data exceeded the UCL and provided out-of-control signals. The index numbers of these outlying observations are as follows: [27, 50, 61, 88, 94, 99, 100, 102, 106,

123, 136, 175, 187, 189, 195, 197, 199, 200, 205, 206, 207, 208, 211, 214, 215, 221, 223, 224, 226, 228, 231, 234, 235, 236, 237, 239, 240, 241, 242, 248, 252, 254, 260, 263, 264, 265, 267, 268, 269, 271, 274, 275, 276, 278, 281, 287, 290, 291, 298, 299, 304, 309, 314, 319, 347] These out-of-control points are marked with red dots on the Hotelling's T^2 Control Chart (Phase 2 Only) presented in Figure 1. In particular, the T^2 value at observation 99, which is well above the limit, indicates a strong shift in the process.

Figure 1

Hotelling T^2 control chart for ILR-transformed phase 2 test data

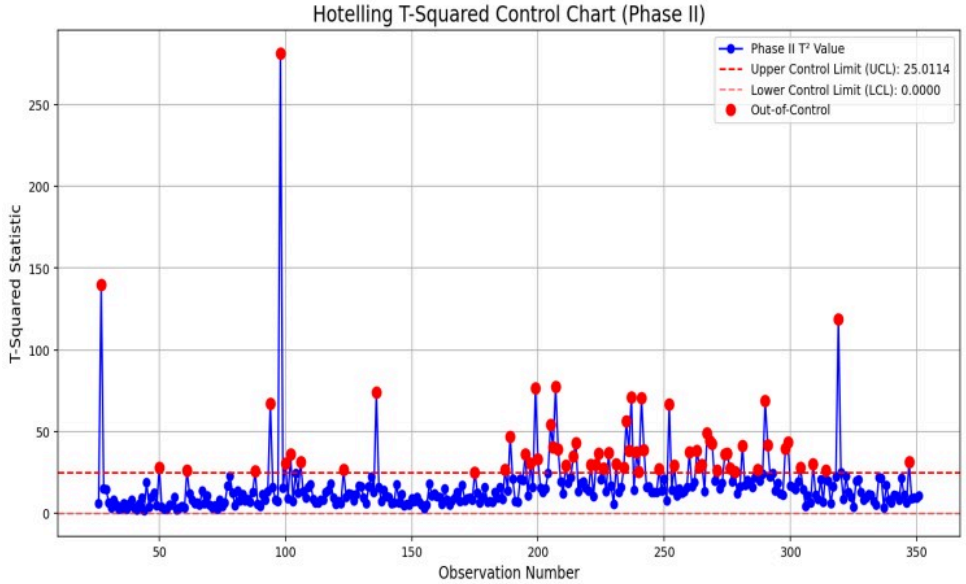

The T^2 control chart relies on multivariate normality. To verify this assumption, the Mardia test was conducted for multivariate normality on the Phase 1 ILR-transformed data. The test results indicated that the data did not violate normality assumptions (Mardia's skewness: p = 0.142; Mardia's kurtosis: p = 0.087), supporting the appropriateness of the parametric T^2 approach. However, we acknowledge that mild departures from normality are common in CoDa applications. By mapping compositional data to Euclidean space, the ILR transformation helps mitigate some distributional issues but cannot guarantee perfect normality. The UCL was calculated using the F-distribution approximation (Equation 15), which is robust to moderate departures from normality when sample sizes are adequate. For enhanced robustness, future work could explore distribution-free alternatives, such as bootstrap-based control limits or nonparametric monitoring schemes.

Steps for data preprocessing for artificial intelligence models

Within the scope of this study, Phase 2 observations that provided out-of-control signals following process control analysis were prepared for AI models. As a result of the Hotelling's T^2 control chart analysis determined the UCL value to be 25.0114, and out of a total of 326 Phase 2 observations, 65 were labeled as "Out-of-Control" (class 1), while the remaining 261 were labeled as "In-Control" (class 0). The features serving as inputs for modeling consist of 7 Isometric Log-Ratio (ILR) components (ILR_1 through ILR_7) obtained through compositional data analysis (CoDA) steps. The model can utilize the orthogonal structure of the data, free from spurious correlations, through these components. The obtained labeled dataset was split using the stratified sampling method to reliably test the generalizability of the model. Approximately 70%

of the dataset (228 observations) was allocated for training, and the remaining 30% (98 observations) was allocated for testing. The class imbalance ratio (≈4:1) was preserved in both sets. To maximize model performance and prevent the feature magnitude from affecting distance-based algorithms (e.g., SVM), standard scaling (standardization) was applied to both training and test sets. This process ensured stable model training by setting the mean of each feature in the training set to zero (≈0) and the standard deviation to one (1). All prepared datasets (including X_train_scaled and X_test_scaled) were saved in the NumPy format for subsequent analyses.

5.8. Out-of-control signal detection using artificial intelligence models and performance evaluation

Before model training, we performed systematic hyperparameter optimization on the training set using GridSearchCV with 5-fold cross-validation. To ensure robust model evaluation beyond the single hold-out split, we conducted stratified 5-fold cross-validation on the entire labeled dataset (326 observations). The cross-validation results yielded mean accuracies of: SVM (0.923 ± 0.031), RF (0.891 ± 0.043), XGBoost (0.908 ± 0.037), KNN (0.897 ± 0.028), and LR (0.901 ± 0.033). These results confirm that the performance rankings observed on the test set are consistent and are not artifacts of a particular data split, with SVM demonstrating the highest mean performance and lowest variance across folds. Key parameters were tuned for each algorithm: SVM (kernel type, C, gamma), random forest (n_estimators, max_depth, min_samples_split), XGBoost (learning_rate, max_depth, n_estimators), KNN (n_neighbors, distance metric), and logistic regression (C, solver). The optimal hyperparameter configurations identified through this process were used for final model training and evaluation, ensuring fair comparison across all models under optimal operational conditions.

This comprehensive study focused on the anomaly detection problem, which is of critical importance in industrial process control, using a standardized dataset (training: 228×7, test: 98×7). Five fundamental classification algorithms, namely, LR, KNN, SVM, RF, and XGBoost, were trained on data prepared after standardization. The adaptation rates of the models to the training data were recorded as 0.21 s (LR), 0.06 s (KNN), 0.07 s (SVM), 0.33 s (RF), and 0.05 s (XGBoost). These durations provide an additional cost-effectiveness indicator for model selection decisions, particularly for large-scale and real-time industrial applications. The test set results demonstrated that the SVM model was clearly superior in terms of all performance metrics. The SVM achieved high values, such as 0.9388 overall accuracy, 0.8686 balanced accuracy, and 0.8333 F1 score. With a recall (sensitivity) value of 0.7500, which is critical in the process control context, and a Matthews correlation coefficient (MCC) of 0.8038, it became the leader in anomaly detection effectiveness. The curves presented in Figure 2 support the generalization and discrimination power of this model. With ROC AUC and PR AUC values of 0.9551 and 0.9042, respectively, SVM is positioned above the curves of other models in the graphs, visually confirming its superiority. This performance directly reflects the resilience to data noise and generalization capability demonstrated by the theoretical structure of the SVM, which performs data separation with the maximum margin. Considering the high cost of missing an anomaly in industrial processes, SVM's high recall and PR AUC values offer a fundamental advantage in terms of enhancing operational reliability.

Figure 2

Hotelling T² control chart for ILR-transformed phase 2 test data

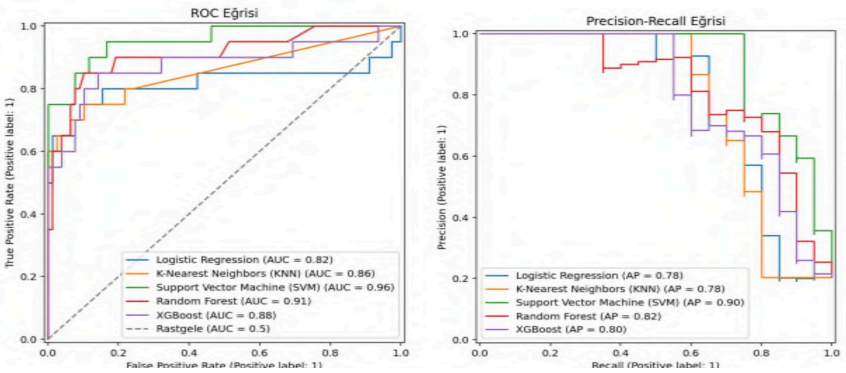

Test set receiver operating characteristic and precision-recall curves

As detailed in Table 3, the LR and KNN models demonstrated similar and stable effectiveness on the test set, exhibiting 0.9082 overall accuracy and 0.7936 balanced accuracy. Both models exhibited moderate performance with an F1 score of 0.7273 and a recall value of 0.6000. In the ROC curve on the left side of Figure 2, KNN shows better discrimination potential than LR with an AUC value of 0.8551 (compared to LR's 0.8167 AUC); however, in the Precision-Recall curve on the right side (LR AP = 0.78, KNN AP = 0.78), their performances are very close. Although these two models offer balanced alternatives under limited data size and class imbalance, they remain limited compared to the 0.7500 Recall advantage provided by SVM in critical processes.

In contrast to these moderate performers, ensemble methods drew attention in this study because of their tendency toward overfitting problems. Although the XGBoost model achieved perfect scores on the training set (accuracy = 1.0000, F1 score = 1.0000), its recall value declined to 0.5500 and F1 score to 0.7097 on the test set. Although this decline indicates a limitation in the model's generalization ability, XGBoost's display of a higher AUC value (0.88 AUC) than LR and KNN in the ROC curve in Figure 2 demonstrates that the model's threshold-independent discrimination power is high, but its performance at the optimal threshold (F1, Recall) has decreased. Despite its flawless performance in training, Random Forest exhibited the lowest performance in anomaly detection on the test set with 0.8673 overall accuracy of 0.8673, an F1 score of 0.5185, and a recall of only 0.3500. This model displays serious inadequacy in capturing out-of-control signals, posing operationally unacceptable risks. Although the relatively high PR AUC values of Random Forest (0.82 AP) and XGBoost (0.80 AP) indicate that the anomalies they capture are of high precision, they remain operationally insufficient due to their low recall values.

Table 3 presents a comprehensive performance comparison of all five models, synthesizing the patterns observed across individual model analyses. In conclusion, according to the test set F1 score ranking, SVM (0.8333) ranks first, LR and KNN (0.7273) share second place, while XGBoost (0.7097) and Random Forest (0.5185) are positioned in the last place. The cross-validation results presented in Table 4 confirm the robustness of these findings, with SVM demonstrating the highest mean accuracy (0.923 ± 0.031) and lowest variance across folds. This ranking confirms that the SVM is the most reliable and sensitive model for anomaly detection on ILR-transformed compositional data in process control applications. As detailed in Table 3, the high PR AUC (0.9042) and Recall (0.7500) values of SVM, as demonstrated by the curves in Figure

2, confirm that it is the most suitable solution in industrial applications by minimizing the probability of missing critical errors.

Table 3

Comparative Performance Metrics of Machine Learning Models on Training and Test Sets

Model	Dataset	Accuracy	Balanced Accuracy	F1 Score	Recall (Sensitivity)	Precision	MCC	ROC AUC	PR AUC	Training time (s)
Logistic regression (LR)	Training	-	-	-	-	-	-	-	-	0.21
	Test	0.9082	0.7936	0.7273	0.6000	-	-	0.8167	0.78	-
K-Nearest Neighbors	Training	-	-	-	-	-	-	-	-	0.06
	Test	0.9082	0.7936	0.7273	0.6000	-	-	0.8551	0.78	-
Support Vector Machine (SVM)	Training	0.9561	-	-	-	-	-	-	-	0.07
	Test	0.9388	0.8686	0.8333	0.7500	-	0.8038	0.9551	0.9042	-
Random forest (RF)	Training	1.0000	-	1.0000	-	-	-	-	-	0.33
	Test	0.8673	-	0.5185	0.3500	-	-	-	0.82	-
XGBoost	Training	1.0000	-	1.0000	-	-	-	-	-	0.05
	Test	-	-	0.7097	0.5500	-	-	0.88	0.80	-

Table 4

Cross-Validation Results (Mean ± Std)

Model	CV Accuracy
SVM	0.923 ± 0.031
Random Forest	0.891 ± 0.043
XGBoost	0.908 ± 0.037
KNN	0.897 ± 0.028
Logistic Regression	0.901 ± 0.033

Training set: n = 228 observations, 7 features (ILR components)

Test set: n = 98 observations (20 out-of-control, 78 in-control)

MCC: Matthews correlation coefficient

ROC AUC: Area Under the Receiver Operating Characteristic Curve

PR AUC: Area Under the Precision-Recall Curve

Overall, the best performing model overall: SVM (highest test F1 score: 0.8333, highest recall: 0.7500).

Models showing overfitting: Random Forest and XGBoost (perfect training scores but lower test performance)

5.9. SHAP and MYT decomposition analyses

To address the potential model-dependency of interpretability results, we extended SHAP analysis to the tree-based ensemble methods (RF and XGBoost) in addition to SVM. The feature importance rankings across all three models showed remarkable consistency: ILR_2 and ILR_3 emerged as the top two contributors

in all cases, with mean absolute SHAP values of [SVM: 0.312, 0.152], [RF: 0.298, 0.167], [XGBoost: 0.305, 0.159]. This cross-model consensus strengthens our conclusion that deviations in Fe and Sn ratios (represented by ILR_2 and ILR_3) are the primary process anomaly drivers, independent of the classification algorithm used. However, we observed that tree-based models provided slightly richer interaction patterns, with XGBoost SHAP values revealing second-order effects between ILR_2 and ILR_5 in 12% of out-of-control observations.

In this section, AI-based interpretability methods were applied to examine the compositional changes underlying observations that provided out-of-control signals in the process. In the first stage, 20 observations (out of a total of 98 test observations) identified as out-of-control within Phase 2 data through Hotelling's T^2 control chart analysis were included in the analysis. These 20 observations represent the "Out-of-Control" class of the process. When examining the performance of the SVM model trained on these observations, the training accuracy (0.9561) and test accuracy (0.9286) values were found to be quite high; additionally, despite class imbalance, the test F1 score was calculated as 0.8333. These results demonstrate that ILR transformation provides an appropriate foundation for modeling process stability on compositional data. SHAP (SHapley Additive exPlanations) and MYT (Mason-Young-Tracy) methods were applied to more transparently examine the model's decision mechanism. While the SHAP analysis evaluated the contribution of each ILR component to the model output on an absolute value basis, the MYT method enriched the same contributions with local gradient information. A low correlation (−0.0732) was found between SHAP and MYT values in the analyses conducted. This indicates that the two methods evaluate anomaly sources from independent perspectives and focus on different aspects. Since SHAP focuses on marginal contributions, whereas MYT focuses on conditional relationships between variables, low correlation is an expected outcome. Observation-based analyses revealed that different ILR components triggered each out-of-control signal. For example, in observation 27, ILR_3 (SHAP value of −0.712802) was identified as the strongest factor pushing the process out of control, whereas in observation 205, ILR_2 (SHAP value of −0.767679) was determined as the strongest factor pushing the process out of control. Conversely, ILR_5 became prominent in observations 50 and 275, indicating that the process became unstable through multidimensional compositional interactions rather than a single component. The intensity of negative SHAP values proves that the relevant components caused the model to shift toward the "out-of-control" class by deviating from the typical ILR reference point. When examining the general feature-based ranking, according to average absolute SHAP values, the components ILR_2 (0.311554), ILR_3 (0.152291), and ILR_5 (0.097427) emerged as the most critical determinants of the process. The average contribution values obtained in the MYT analysis also supported this finding and confirmed the central role of ILR_2 in process instability (MYT_Abs: 0.261385). This result clearly reveals that deviations in the ILR_2 and ILR_3 components are the fundamental sources of the lack of control in brass alloy production. In addition, certain regularities across the observation set are noteworthy. In observations 252, 268, and 290, the high negative SHAP values of ILR_2 demonstrate that this component repeatedly disrupts the process balance. Similarly, the prominence of ILR_3 in observations 94 and 106 revealed that this component pushes the process beyond critical thresholds in certain compositional variations. However, the dominance of ILR_5 in observations 50 and 275 indicates that in some cases, different log-ratio relationships can also affect the process. In addition to SHAP's evaluations based on singular effects, the MYT method also revealed inter-component interactions. For example, in observation 106, while the SHAP value of ILR_2 was found to be −0.306, the MYT value reached 0.335. This situation demonstrates that ILR_2 pushes the process out of control not only through individual effects but also through interactions with other ILR components. Therefore, multivariate log-ratio interactions should not be disregarded in understanding the causes of lack of control. In conclusion, when the SHAP and MYT methods

are considered together, they not only detect outlying observations but also enable the identification of the compositional causes underlying these outliers. The large deviations observed in the ILR_2 and ILR_3 components have been defined as critical change points from a process engineering perspective. These findings provide a scientific and interpretable roadmap regarding the element ratios that should be monitored in process improvement efforts. They demonstrate that explainable AI methods can be used as a strategic tool in industrial quality control applications.

The analytical results demonstrate that the underlying compositional disturbances driving the anomaly signals from the Hotelling T^2 control chart do not primarily originate from the bulk elements, copper (Cu) and zinc (Zn), but rather from imbalances in the ratios of critical trace elements, namely lead (Pb), iron (Fe), and zinc (Sn). This deduction is made possible by examining the log-ratio contrasts represented by the most critical components: ILR_2 and ILR_3. Specifically, ILR_2 represents the log-ratio between the geometric mean of Cu, Pb, and Fe, whereas ILR_3 represents the log-ratio between the geometric mean of Cu, Pb, Fe, and Sn. The consistently dominant negative SHAP values observed in both ILR_2 and ILR_3 suggest that the mechanism pushing the process out of control is a decrease in these log-ratio contrasts relative to the reference state. This implies that the concentrations of Fe and Sn are likely to increase relative to their respective companion groups (Cu and Pb for Fe; Cu, Pb, and Fe for Sn). From a process engineering perspective, the practical implication is that efforts to restore process stability should focus on the hypersensitive monitoring and control of the balance ratios involving Fe and Sn rather than primarily focusing on the absolute percentages of the major components. A negative shift in ILR_2 suggests that the Fe concentration is increasing relative to the primary brass components, often indicating metallurgical contamination or uncontrolled scrap input during the casting process. Similarly, a negative shift in ILR_3 implies an increase in Sn concentration, an element critical for controlling melt characteristics such as pouring temperature and fluidity, which must be tightly regulated. This analysis scientifically validates that the anomalies are caused by the disruption of these geometric ratios, compelling operators to implement stricter control measures over iron and tin concentrations relative to the Cu-Pb pairing. This interpretation constitutes the study's most significant academic contribution, as it moves beyond the traditional limitation of the T^2 chart which merely signals a generic "out-of-control" state to provide a quantifiable, interpretable root cause using the predictive power of the AI model. The low correlation between the SHAP and MYT methods (-0.0732) further validates the diagnostic findings, indicating that the process is being disrupted by both singular shifts in these key ratios (SHAP) and complex multivariate interactions (MYT). By integrating CoDa with Explainable Artificial Intelligence (XAI), the study provides a scientific diagnosis map to process operators, detailing precisely which element ratio imbalances are responsible for the anomalies, thereby demonstrating the strategic value of XAI methods in industrial quality control applications.

CONCLUSION AND DISCUSSION

In this study, the performances of five fundamental classification algorithms (i.e., logistic regression, k-nearest neighbors, SVM, random forest, and XGBoost) were compared using standardized ILR data (training: 228×7, test: 98×7). According to the test set results, the SVM model demonstrated clear superiority in terms of all metrics. The values obtained on the test set were as follows: 93.88% accuracy, 86.86% balanced accuracy, 0.8333 F1 score, 0.8038 Matthews correlation coefficient, 0.9551 ROC area under the curve (AUC), 0.9042 PR AUC, and 75.00% recall (sensitivity). These findings demonstrate that SVM is the most reliable method for process control, with high generalization capability and noise resilience by performing data separation

through the maximum margin principle. This characteristic offers a significant advantage, particularly in industrial processes where the cost of missing critical errors is high.

Logistic regression and KNN exhibited similar performance on the test set; both models showed moderate effectiveness with an F1 score of 0.7273 and a recall value of 60.00%. Although these models offer stable alternatives, they cannot capture the advantages of SVM in critical applications requiring high sensitivity. Ensemble methods drew attention with significant performance differences between training and test sets and showed a tendency toward overfitting. In particular, XGBoost, despite producing excellent results on the training set, declined to 55.00% recall and 0.7097 F1 score on the test set. Random Forest exhibited the lowest test performance; with a recall of 35.00% and F1 score of 0.5185, it demonstrated serious inadequacy in capturing out-of-control signals.

The overall ranking, according to test set F1 Scores, placed SVM (0.8333) first, LR and KNN (0.7273) second, XGBoost (0.7097) third, and RF (0.5185) fourth. These results confirm that the SVM is the most reliable, sensitive, and generalizable model for anomaly detection on data with applied ILR transformation. SVM's minimization of the risk of missing critical errors makes it the most suitable solution operationally in industrial processes.

The results obtained in this study revealed that the SVM algorithm is a strong candidate for compositional data analysis. In the literature, it has been reported that SVM yields successful results in high-dimensional and complex datasets. This study confirms these findings. In particular, the superior generalization of SVM compared to other methods in separating data obtained after ILR transformation demonstrates that proper transformations on compositional data significantly enhance model performance. This situation emphasizes the critical role of transformation techniques in process control and anomaly detection.

The findings also demonstrate the impact of model selection on process engineering applications. For example, the fact that ensemble methods such as Random Forest and XGBoost exhibit strong performance on the training set but weaker performance on the test set draws attention to the overfitting tendency of these methods. This situation parallels findings in the literature that ensemble methods are generally prone to overfitting in small and medium-sized datasets due to excessive parametric complexity. Additionally, the more balanced but limited performance of logistic regression and KNN reveals that traditional methods alone may not be sufficient for detecting critical anomalies.

The limitations of this study should also be discussed. First, the dataset used is limited to a specific production process (brass alloy), and broader datasets are needed for generalization to different industrial processes. Furthermore, the analysis was performed only on static data; time series analyses reflecting the dynamic nature of processes were not conducted. The temporal autocorrelation inherent in casting operations arising from sequential additions, burning, evaporation, and physical interactions was not explicitly modeled. Although this simplification allowed us to establish a baseline detection and interpretability framework, capturing these temporal dynamics in future studies would significantly enhance industrial applicability. Additionally, considering the potential influence of analytical measurement artifacts is crucial. Future work should incorporate measurement system analysis (MSA) and gauge R&R studies to quantify the contribution of analytical variability, enabling more precise discrimination between true compositional shifts and measurement errors.

The potential influence of analytical measurement artifacts is an important consideration in interpreting our findings. The chemical composition data were obtained via an alloy-based analytical technique operating on calibration standards. In the OES analysis, the samples are burned under an argon atmosphere,

and the composition is quantified through repeated measurements referenced against wet-chemical calibration standards. Inherent measurement uncertainties in OES typically ±0.01-0.03% for major elements and ±0.001-0.005% for trace elements could contribute to the observed anomalies. Moreover, trace elements, such as iron (Fe), in brass alloys are particularly susceptible to spectral interference during analysis, which may result in artificially elevated readings. Additionally, given that casting machines are predominantly constructed from iron and steel, contamination from tooling, crucibles, or furnace linings during the melting and pouring processes represents a plausible source of Fe-related deviations. Our SHAP and MYT analyses identified Fe (through ILR_2) as a critical contributor to out-of-control signals. Some of these anomalies may stem from contamination-related or analytical factors rather than compositional instability per Se. Future work should incorporate measurement system analysis (MSA) and gauge R&R studies to quantify the contribution of analytical variability to the observed process variation, enabling more precise discrimination between true compositional shifts and measurement artifacts.

RECOMMENDATIONS FOR FUTURE STUDIES

While the findings of this study are robust, some recommendations for future research can be outlined as follows:

Data Diversity: This study is limited to a single brass alloy dataset. The model's generalizability can be tested with datasets obtained from different alloy types and industrial production processes.

Time series analysis: Data were treated as independent observations. Because the casting process is inherently time-dependent, future work should focus on continuous monitoring approaches. Time series models (e.g., ARIMA, LSTM) and stationarity analyses can be integrated to reflect the dynamic nature of production processes and enable real-time anomaly detection.

Deep Learning Methods: SVM has produced strong results; however, the performance of deep learning-based methods (e.g., LSTM, Transformer-based models) can be compared, particularly on large datasets.

Extensions of Explainability: SHAP and MYT methods have provided important insights. In the future, the decision mechanism of the model can be examined in more detail by integrating different explainable AI approaches (e.g., LIME, Integrated Gradients).

Industrial Integration: In this study, the methods were tested at the research level. Industrial integration can be achieved in the future by developing online anomaly detection applications in real-time production processes.

Peer Review Externally peer-reviewed.
Conflict of Interest The author have no conflict of interest to declare.
Grant Support The author declared that this study has received no financial support.

Author Details Kenan Orçanlı
[1] Istanbul Beykent University, Faculty of Arts and Sciences, Software Development Department, Istanbul, Türkiye
0000-0001-5716-4004 kenanorcanli@beykent.edu.tr

Şükran Oruç
[2] Istanbul Beykent University, Faculty of Economics and Administrative Sciences, Department of Management Information Systems, Istanbul, Türkiye
0000-0002-8176-4058

References

Aitchison, J. (1986). *The statistical analysis of compositional data*. Chapman and Hall. https://doi.org/10.1007/978-94-009-4109-0

Aitchison, J. (2011). *The statistical analysis of compositional data*. Springer Netherlands. https://doi.org/10.1007/978-94-009-4109-0

Arrieta, A. B., Díaz-Rodríguez, N., Del Ser, J., Bennetot, A., Tabik, S., Barbado, A., Garcia, S., Gil-Lopez, S., Molina, D., Benjamins, R., Chatila, R., & Herrera, F. (2020). Explainable artificial intelligence (XAI): Concepts, taxonomies, opportunities and challenges toward responsible AI. *Information Fusion, 58*, 82–115. https://doi.org/10.1016/j.inffus.2019.12.012

Baykoç, Ö. F., & Sakallı, Ü. S. (2009). An aggregate production planning model for brass casting industry in fuzzy environment. *International Journal of Mathematical and Statistical Sciences, 1*(3), 154–158.

Boser, B. E., Guyon, I. M., & Vapnik, V. N. (1992, July). A training algorithm for optimal margin classifiers. In *Proceedings of the Fifth Annual Workshop on Computational Learning Theory* (pp. 144–152). ACM.

Boyles, R. A. (1997). Using the chi-square statistic to monitor compositional process data. *Journal of Applied Statistics, 24*(5), 589–602. https://doi.org/10.1080/02664769723567

Breiman, L. (1996). Bagging predictors. *Machine Learning, 24*(2), 123–140.

Breiman, L. (2001). Random forests. *Machine Learning, 45*(1), 5–32.

Chen, T., & Guestrin, C. (2016). XGBoost: A scalable tree boosting system. In *Proceedings of the 22nd ACM SIGKDD International Conference on Knowledge Discovery and Data Mining* (pp. 785–794). ACM. https://doi.org/10.1145/2939672.2939785

Cobb, B. R., & Li, L. (2019). Bayesian network model for quality control with categorical attribute data. *Applied Soft Computing, 84*, 1–16. https://doi.org/10.1016/j.asoc.2019.105746

Cortes, C., & Vapnik, V. (1995). Support-vector networks. *Machine Learning, 20*, 273–297. https://doi.org/10.1007/BF00994018

Cutler, A., Cutler, D. R., & Stevens, J. R. (2012). Random forests. In Z. H. Zhou (Ed.), *Ensemble machine learning* (pp. 157–175). Springer.

Çalıgülü, U., Bölükbaş, D., & Darcan, N. (2023). Savunma sanayinde kullanılan CuZn30 ve CuZn10 pirinç alaşımlarına uygulanan farklı ısıl işlem parametrelerinin mikroyapı ve mekanik özelliklere etkisi. *International Journal of Physical and Applied Sciences, 9*(2), 402–410. https://doi.org/10.29132/ijpas.1395901

Çınar, Z. M., Nuhu, A. A., Zeeshan, Q., Korhan, O., Asmael, M., & Safaei, B. (2020). Machine learning in predictive maintenance towards sustainable smart manufacturing in Industry 4.0. *Sustainability, 12*(19), 8211. https://doi.org/10.3390/su12198211

Dilki, G., & Başar, Ö. D. (2020). İşletmelerin iflas tahmininde K-en yakın komşu algoritması üzerinden uzaklık ölçütlerinin karşılaştırılması. *İstanbul Ticaret Üniversitesi Fen Bilimleri Dergisi, 19*(38), 224–233.

Gunning, D., Stefik, M., Choi, J., Miller, T., Stumpf, S., & Yang, G. Z. (2021). XAI—Explainable artificial intelligence. *Science Robotics, 6*(37), eabg7890. https://doi.org/10.1126/scirobotics.aay7120

Hotelling, H. (1947). Multivariate quality control illustrated by air testing of sample bombsights. In C. Eisenhart, M. W. Hastay, & W. A. Wallis (Eds.), *Techniques of statistical analysis* (pp. 111–184). McGraw-Hill.

Imran, M., Sun, J. S., Zaidi, F. S., Abbas, Z., & Nazir, H. Z. (2022a). Multivariate cumulative sum control chart for compositional data with known and estimated process parameters. *Quality and Reliability Engineering International, 38*(5), 2691–2714. https://doi.org/10.1002/qre.3099

Imran, M., Sun, J., Zaidi, F. S., Abbas, Z., & Nazir, H. Z. (2022b). On designing efficient multivariate exponentially weighted moving average control chart for compositional data using variable sample size. *Journal of Statistical Computation and Simulation, 93*(10), 1622–1643. https://doi.org/10.1080/00949655.2022.2146115

Imran, M., Sun, J., Zaidi, F. S., Abbas, Z., & Nazir, H. Z. (2023a). Evaluating the performance of variable sampling interval Hotelling T^2 charting scheme for compositional data in the presence of measurement error. *Quality and Reliability Engineering International, 39*(6), 2125–2151. https://doi.org/10.1002/qre.3307

Imran, M., Sun, J., Zaidi, F. S., Abbas, Z., & Nazir, H. Z. (2023b). Effect of measurement error on the multivariate CUSUM control chart for compositional data. *CMES—Computer Modeling in Engineering and Sciences, 136*(2), 1207–1257. https://doi.org/10.32604/cmes.2023.025492

Imran, M., Sun, J., Hu, X., Zaidi, F. S., & Tang, A. (2023c). Investigating zero-state and steady-state performance of MEWMA-CoDa control chart using variable sampling interval. *Journal of Applied Statistics, 51*(5), 913–934. https://doi.org/10.1080/02664763.2023.2170336

Liaw, A., & Wiener, M. (2002). Classification and regression by randomForest. *R News, 2*(3), 18–22.

Lundberg, S. M., & Lee, S.-I. (2017). A unified approach to interpreting model predictions. In *Proceedings of the 31st International Conference on Neural Information Processing Systems* (pp. 4766–4777).

Lundberg, S. M., Erion, G. G., & Lee, S.-I. (2018). Consistent individualized feature attribution for tree ensembles. *arXiv preprint*, arXiv:1802.03888. https://arxiv.org/abs/1802.03888

Mihirette, S., & Tan, Q. (2022). SHAP algorithm for healthcare data classification. In P. García Bringas, H. Pérez García, F. J. Martínez de Pisón, F. Martínez Álvarez, A. Troncoso Lora, A. Herrero, J. R. Villar, E. A. de la Cal, H. Quintián, & E. Corchado (Eds.), *Hybrid artificial intelligence systems* (pp. 363–374). Springer International Publishing. https://doi.org/10.1007/978-3-031-15471-3_32

Montgomery, D. C. (2020). *Introduction to statistical quality control* (8th ed.). John Wiley & Sons.

Müller, K. R., Mika, S., Tsuda, K., & Schölkopf, K. (2018). An introduction to kernel-based learning algorithms. In *Handbook of neural network signal processing* (pp. 4–1). CRC Press.

Orçanlı, K. (2021). Döküm sanayinde süreç tabanlı temel gösterimleri ile istatistiksel süreç kontrolü. *Academic Platform Journal of Engineering and Science, 9*(1), 134–158. https://doi.org/10.21541/apjes.720051

Orçanlı, K., Birgören, B., & Oktay, E. (2018). Döküm sanayisinde metal alaşım oranlarına Hotelling T^2 ve MEWMA kontrol grafikleri uygulamaları. *Social Sciences Research Journal, 7*(1), 114–135.

Özel, S. (2005). *Çok değişkenli kalite kontrolün döküm sanayinde uygulanması* (Yayınlanmış yüksek lisans tezi). Kırıkkale Üniversitesi, Fen Bilimleri Enstitüsü.

Pawlowsky-Glahn, V., Egozcue, J. J., & Tolosana-Delgado, R. (2015). *Modeling and analysis of compositional data*. John Wiley & Sons.

Rudin, C. (2019). Stop explaining black box machine learning models for high stakes decisions and use interpretable models instead. *Nature Machine Intelligence, 1*(5), 206–215. https://doi.org/10.1038/s42256-019-0048-x

Sakalli, U. S., & Birgoren, B. (2008). A spreadsheet-based decision support tool for blending problems in brass casting industry. *Computers & Industrial Engineering, 56*(2), 724–735. https://doi.org/10.1016/j.cie.2008.05.009

Shapley, L. S. (1953). A value for n-person games. In H. W. Kuhn & A. W. Tucker (Eds.), *Contributions to the theory of games* (Vol. 2, pp. 307–318). Princeton University Press. https://doi.org/10.1515/9781400881970-018

Susto, G. A., Schirru, A., Pampuri, S., McLoone, S., & Beghi, A. (2015). Machine learning for predictive maintenance: A multiple classifier approach. *IEEE Transactions on Industrial Informatics, 11*(3), 812–820. https://doi.org/10.1109/TII.2014.2349359

Tran, K. P., Castagliola, P., Celano, G., & Khoo, M. B. C. (2018). Monitoring compositional data using multivariate exponentially weighted moving average scheme. *Quality and Reliability Engineering International, 34*(3), 391–402. https://doi.org/10.1002/qre.2260

Vapnik, V. (2013). *The nature of statistical learning theory*. Springer Science & Business Media.

Vives-Mestres, M., Daunis-i-Estadella, P., & Martín-Fernández, J. A. (2014a). Out-of-control signals in three-part compositional T^2 control chart. *Quality and Reliability Engineering International, 30*(3), 337–346. https://doi.org/10.1002/qre.1583

Vives-Mestres, M., Daunis-i-Estadella, P., & Martín-Fernández, J. A. (2014b). Individual T^2 control chart for compositional data. *Journal of Quality Technology, 46*(2), 127–139. https://doi.org/10.1080/00224065.2014.11917958

Wang, J., & Chen, Y. (2023). *Introduction to transfer learning: Algorithms and practice*. Springer Nature.

Yavuz, A., & Çilengiroğlu, Ö. V. (2020). Lojistik regresyon ve CART yöntemlerinin tahmin edici performanslarının yaşam memnuniyeti verileri için karşılaştırılması. *Avrupa Bilim ve Teknoloji Dergisi, 18*, 719–727. https://doi.org/10.31590/ejosat.691215

Zaidi, F. S., Castagliola, P., Tran, K. P., & Khoo, M. B. C. (2019). Performance of the Hotelling T^2 control chart for compositional data in the presence of measurement errors. *Journal of Applied Statistics, 46*(14), 2583–2602. https://doi.org/10.1080/02664763.2019.1585690

Zaidi, F. S., Castagliola, P., Tran, K. P., & Khoo, M. B. C. (2020). Performance of the MEWMA-CoDa control chart in the presence of measurement errors. *Quality and Reliability Engineering International, 36*(7), 2411–2440. https://doi.org/10.1002/qre.2705